Discovery of the optical counterpart and early optical observations of GRB 990712

Sahu, K.C.; Vreeswijk, P.M.; Bakos, G.; Menzies, J.W.; Bragaglia, A.; Frontera, F.; Piro, L.; Albrow, M.D.; Bond, I.A.; Bower, R.; Caldwell, J.A.R.; Castro-Tirado, A.J.; Courbin, F.; Dominik, M.; Fynbo, J.U.; Galama, T.J.; Glazebrook, K.; Greenhill, J.; Gorosabel, J.; Hearnshaw, J.; Hill, K.; Hjorth, J.; Kane, S.; Kilmartin, P.M.; Kouveliotou, C.; Martin, R.; Masetti, N.; Maxted, P.; Minniti, D.; Moslashiller, P.; Muraki, Y.; Nakamura, T.; Noda, S.; Ohnisi, K.; Palazzi, E.; van Paradijs, J.A.; Pian, E.; Pollard, K.; Rattenbury, N.J.; Reid, M.; Rol, E.; Saito, T.; Sackett, P.D.; Saizar, P.; Tinney, C.; Vermaak, P.; Watson, R.; Williams, A.; Yock, P.; Dar, A.

Published in:
Astrophysical Journal

DOI:
10.1086/309340

THE ASTROPHYSICAL JOURNAL, 540:74–80, 2000 September 1

DISCOVERY OF THE OPTICAL COUNTERPART AND EARLY OPTICAL OBSERVATIONS OF GRB 990712[1]

K. C. SAHU,[2] P. VREESWIJK,[3] G. BAKOS,[2,4] J. W. MENZIES,[5] A. BRAGAGLIA,[6] F. FRONTERA,[7] L. PIRO,[8] M. D. ALBROW,[9] I. A. BOND,[10] R. BOWER,[11] J. A. R. CALDWELL,[5] A. J. CASTRO-TIRADO,[12,13] F. COURBIN,[14] M. DOMINIK,[15] J. U. FYNBO,[16] T. GALAMA,[3,17] K. GLAZEBROOK,[18] J. GREENHILL,[19] J. GOROSABEL,[12] J. HEARNSHAW,[9] K. HILL,[19] J. HJORTH,[20] S. KANE,[19] P. M. KILMARTIN,[9] C. KOUVELIOTOU,[21] R. MARTIN,[22] N. MASETTI,[7] P. MAXTED,[23] D. MINNITI,[14] P. MØLLER,[24] Y. MURAKI,[25] T. NAKAMURA,[26] S. NODA,[25] K. OHNISHI,[27] E. PALAZZI,[7] J. VAN PARADIJS,[3,28] E. PIAN,[7] K. R. POLLARD,[9] N. J. RATTENBURY,[10] M. REID,[29] E. ROL,[3] T. SAITO,[30] P. D. SACKETT,[15,18] P. SAIZAR,[31] C. TINNEY,[18] P. VERMAAK,[5] R. WATSON,[19] A. WILLIAMS,[22] P. YOCK,[10] AND A. DAR[33]

Received 1999 December 13; accepted 2000 April 13

ABSTRACT

We present the discovery observations of the optical counterpart of the gamma-ray burst GRB 990712 taken 4.16 hr after the outburst and discuss its light curve observed in the V, R, and I bands during the first $\sim$35 days after the outburst. The observed light curves were fitted with a power-law decay for the optical transient (OT), plus an additional component that was treated in two different ways. First, the additional component was assumed to be an underlying galaxy of constant brightness. The resulting slope of the decay is $0.97^{+0.05}_{-0.02}$, and the magnitudes of the underlying galaxy are $V = 22.3 \pm 0.05$, $R = 21.75 \pm 0.05$, and $I = 21.35 \pm 0.05$. Second, the additional component was assumed to be a galaxy plus an underlying supernova with a time-variable brightness identical to that of GRB 980425, appropriately scaled to the redshift of GRB 990712. The resulting slope of the decay is similar, but the goodness of fit is worse, which would imply that either this GRB is not associated with an underlying supernova or the underlying supernova is much fainter than the supernova associated with GRB 980425. The galaxy in this case is fainter: $V = 22.7 \pm 0.05$, $R = 22.25 \pm 0.05$, and $I = 22.15 \pm 0.05$, and the OT plus the underlying supernova at a given time is brighter. Measurements of the brightnesses of the OT and the galaxy by late-time *Hubble Space Telescope* observation and ground-based observations can thus assess the presence of an underlying supernova.

Subject headings: cosmology: observations — gamma rays: bursts

[1] Based on observations collected at SAAO, Sutherland; ESO, Paranal and La Silla (ESO Programs 63.O-0618 and 63-O-0567); and AAT, Australia.

[2] Space Telescope Science Institute, 3700 San Martin Drive, Baltimore, MD 21218; ksahu@stsci.edu.
[3] Astronomical Institute "Anton Pannekoek," University of Amsterdam, Kruislaan 403, 1098 SJ Amsterdam, The Netherlands.
[4] Konkoly Observatory, P.O. Box 67, 1525 Budapest, Hungary.
[5] South African Astronomical Observatory, P.O. Box 9, Observatory 7935, South Africa.
[6] Osservatorio Astronomico di Bologna, via Ranzani, 40127 Bologna, Italy.
[7] Istituto Te.S.R.E., via Gobetti, 40129 Bologna, Italy.
[8] Istituto di Astrofisica Spaziale, CNR, Rome, Italy.
[9] Department of Physics and Astronomy, University of Canterbury, Private Bag 4800, Christchurch, New Zealand.
[10] Faculty of Science, University of Auckland, New Zealand.
[11] Department of Physics, University of Durham, South Road, Durham DH1 3LE, England, UK.
[12] LAEFF-INTA, P.O. Box 50727, 28080 Madrid, Spain.
[13] Instituto de Astrofísica de Andalucía (IAA-CSIC), P.O. Box 03004, 18080 Granada, Spain.
[14] Department of Astronomy, P. Universidad Católica, Casilla 306, Santiago 22, Chile.
[15] Kapteyn Astronomical Institute, Postbus 800, 9700 AV Groningen, The Netherlands.
[16] Institute of Physics and Astronomy, University of Århus, 8000 Århus C, Denmark.
[17] Palomar Observatory 105-24, Caltech, Pasadena, CA 91125.
[18] Anglo-Australian Observatory, P.O. Box 296, Epping, NSW 2121, Australia.
[19] Physics Department, University of Tasmania, G.P.O. 252C, Hobart, Tasmania 7001, Australia.
[20] Astronomical Observatory, University of Copenhagen, Juliane Maries Vej 30, 2100 Copenhagen, Denmark.
[21] Universities Space Research Association, NASA Marshall Space Flight Center, SD50, Huntsville, AL 35812.
[22] Perth Observatory, Walnut Road, Bickley, Perth 6076, Australia.
[23] Department of Physics and Astronomy, University of Southampton, Highfield, Southampton SO17 1BJ.
[24] European Southern Observatory, Karl-Schwarzschild-Straße 2 85748, Garching bei München, Germany.
[25] Solar-Terrestrial Environment Laboratory, Nagoya University, Furocho, Chikusa-ku, Nagoya 464-8601, Japan.
[26] Yukawa Institute, Kyoto University, Japan.
[27] Nagano National College of Technology, Japan.
[28] Physics Department, University of Alabama in Huntsville, Huntsville, Alabama 35899.
[29] Department of Physics, Victoria University of Wellington, New Zealand.
[30] Tokyo Metropolitan College of Aeronautics, Japan.
[31] Lincoln University College, Buenos Aires, Argentina.
[32] Department of Physics and Space Research Institute, Technion, Haifa 32000, Israel.

1. INTRODUCTION

In the past two years we have witnessed tremendous progress in our understanding of gamma-ray burst (GRB) phenomena. Thanks to the ability of *BeppoSAX* to provide arcminute-sized error boxes for the bursts, the first optical counterpart was detected in 1997 February for GRB 970228 (van Paradijs et al. 1997; Costa et al. 1997). The *Hubble Space Telescope* (*HST*) observations of this GRB provided the first clear indication that the GRB is associated with an external galaxy and is unrelated to its nuclear activity (Sahu et al. 1997a). Shortly thereafter, the redshift measurement of GRB 970508 proved beyond a doubt that GRBs are extragalactic in nature (Metzger et al. 1997; Djorgovski et al. 1997). More than a dozen GRB optical counterparts have been detected since then, with redshifts as high as 3.42 in the case of GRB 971214 (Kulkarni et al. 1998).

The extensive observations of GRB afterglows in X-ray, optical, and radio wavelengths have been shown to be consistent with cosmological fireball models (e.g., Paczyński & Rhoads 1993; Mészáros & Rees 1997; Wijers, Rees, & Mészáros 1997). However, the exact cause of the GRBs has remained elusive, and progress in determining the actual mechanism causing the bursts has been slow. The two leading models for GRBs involve the collapse of a massive star (e.g., Woosley 1996; Paczyński 1998) and the merging of a neutron star with either another neutron star or a black hole (e.g., Eichler et al. 1989; Narayan, Paczyński, & Piran 1992; Sahu et al. 1997b). The "isotropic equivalent energy" of some GRBs is as high as 10^{54} ergs, which exceeds the energy equivalent of the total mass involved in the latter model and hence is thought to favor the former. However, the beaming factor of the emission of the GRB in different wave bands can be high (in both models), so the energetics alone may not be conclusive in favoring one of the models over the other. Since the lifetime of a very massive star is of the order of a million years or shorter, the GRBs are expected to be within or close to star-forming regions in the massive star collapse model. On the other hand, since the kick velocity of a newly formed neutron star is of the order of 200 km s^{-1}, and since the neutron star, on average, is already about 10^8 yr old at the time of the burst, GRBs are generally expected to be far from star-forming regions in the merging neutron star model (Bloom, Sigurdsson, & Pols 1999). Thus, the location of the GRB with respect to the star-forming regions in the host galaxy could be a distinguishing feature that can help in settling the question of the cause of the GRBs. However, if the presence of dense interstellar material is prerequisite for the onset of the optical afterglow, then optical transients (OTs) would be observed *only* in star-forming regions, regardless of whether GRBs result from neutron star mergers or from the collapse of massive stars. In any case, if some OTs are found far away from star-forming regions, the neutron star merger model would be favored. If all OTs are found in star-forming regions, the situation is less clear, and, depending on the model, one may need to investigate other aspects to find distinguishing features. For example, one consequence of the massive star collapse model is that the GRB should be accompanied by an underlying supernova whose brightness variation is distinct from the power-law decay behavior of the OT and may be detectable.

There is a clear bimodality in the observed burst durations: long bursts have timescales of about 10–200 s, and short bursts have timescales of 0.1–1 s (Kouveliotou et al. 1995). All the afterglows that have been discovered so far belong to the subgroup with long bursts (Fishman 1999). All the OTs for which the host galaxies have been observed—although this sample is small—are found to be in galaxies whose spectral indicators suggest star-forming activity (e.g., Fruchter et al. 1999). So there is an interesting possibility that the long-duration GRBs are caused by the collapse of rapidly rotating massive stars, and hence they occur in star-forming regions. The short-duration bursts may be of a different origin and may be caused by the coalescence of two neutron stars. The detection of optical counterparts of short-duration bursts and their observation would be important in order to understand this scenario better.

GRB 990712, being at $z = 0.434$ (Galama et al. 1999; Hjorth et al. 2000), is one of the closest GRBs observed so far and hence provides a good opportunity to determine the possible presence of an underlying supernova, the location of the GRB within the galaxy, and the luminosity of the galaxy in different wave bands. In this paper we present the optical observations of GRB 990712 leading to the discovery of its optical counterpart and subsequent optical imaging observations taken in different filters during the first ~ 35 days after the burst.

2. OBSERVATIONS

GRB 990712 was simultaneously detected on 1999 July 12.69655 with the Gamma-Ray Burst Monitor and the WFC unit 2 on board the *BeppoSAX* satellite. The burst lasted for about 30 s in both the gamma-ray (40–700 keV) and X-ray (2–26 keV) energy ranges and had a double-peaked structure. While its intensity in gamma rays is moderate, it exhibited the strongest X-ray prompt emission observed to date (Heise et al. 1999).

The initial *BeppoSAX* position, with an error circle of 5′ radius, was revised to one with an error radius of only 2′. Our first observations were made at the latter position with the SAAO 1 m telescope at Sutherland, South Africa on 1999 July 12.87 UT, about 4.16 hr after the burst during time generally dedicated to PLANET microlensing observations (Albrow et al. 1998). The optical image was taken through an R filter, with an integration time of 900 s. The detector was a 1024×1024 SITe CCD with an image scale of 0.″309 per pixel and a total field of view of 5.′3 × 5.′3. Comparison of the image with the Digitized Sky Survey (DSS) image for the same field showed the presence of a new source well above the sky background that was absent in the DSS image. This new source had a brightness of $R = 19.4 \pm 0.1$ mag, which is about 2 mag brighter than the limiting magnitude of the DSS image, indicating that the new source was the optical counterpart of the GRB (Bakos et al. 1999a, 1999b). Figure 1 shows the discovery image along with the DSS image taken of the same region. Also marked in the figure are the reference stars used for photometric calibration of the OT. A spectrum of this source obtained a few hours later revealed emission and absorption lines that were used to derive a redshift of 0.434 for this source (Galama et al. 1999). Subsequent observations by various groups showed the decaying nature of this source, further confirming the identification of the OT with the GRB.

We continued the observations with a multiwavelength optical follow-up campaign using the telescopes at SAAO,

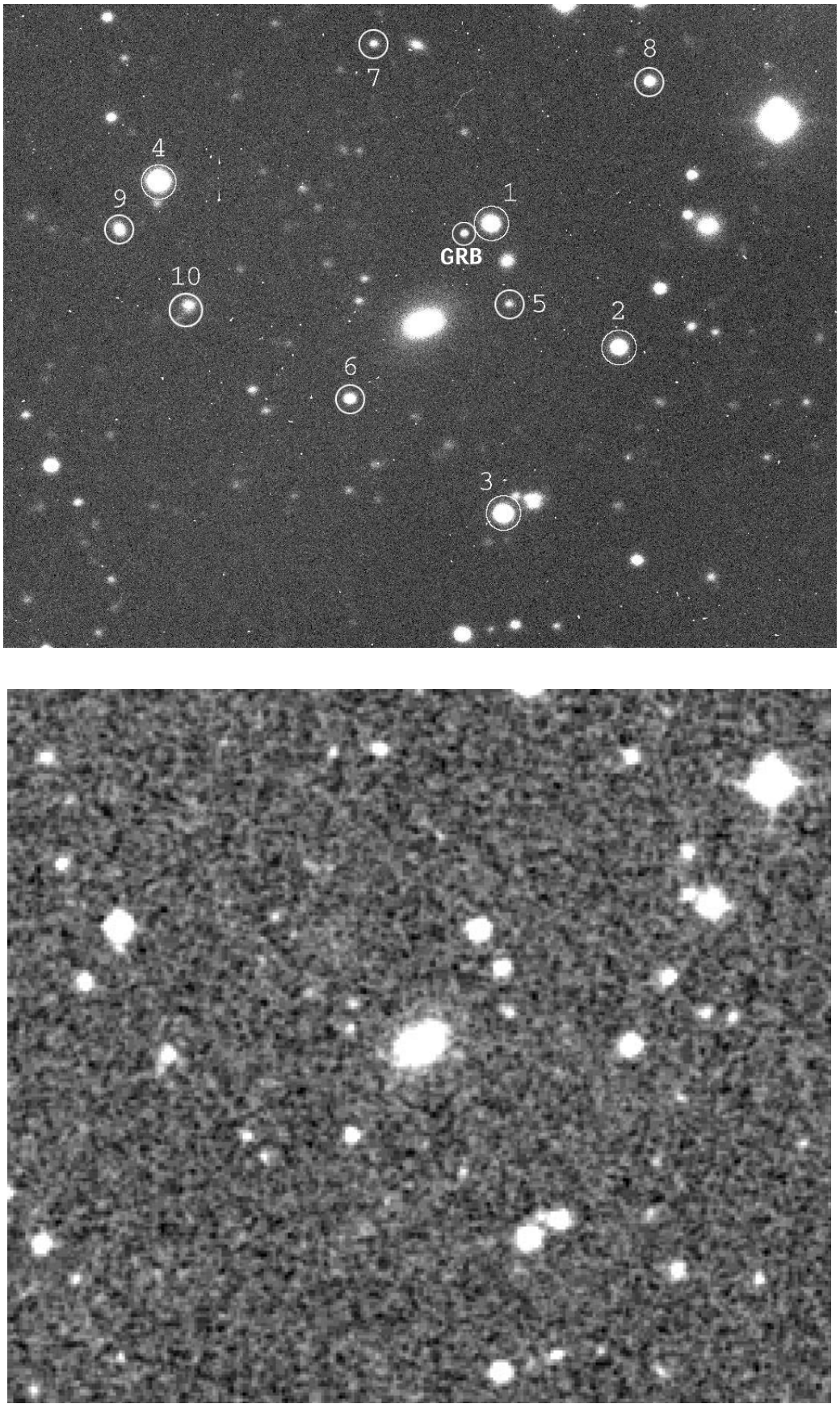

FIG. 1.—Top panel shows the discovery image of the optical counterpart of GRB 990712, obtained with the SAAO 1 m telescope about 4.16 hr after the burst. The bottom panel shows the DSS 3′ × 2.′8 image of the same field. The SAAO image shows the optical counterpart (marked "GRB") as a new source, which is about 2 mag brighter than the limiting magnitude of the DSS image. The reference stars marked 1 and 2 were used as secondary photometric standards, and the reference stars 1–10 were used for the astrometry. North is up and east is to the left.

TABLE 1

JOURNAL OF OBSERVATIONS

Day (1999 UT)	Magnitude	Telescope
R-Band Measurements		
Jul 12.873	19.349 ± 0.019	SAAO 1 m
Jul 13.129	20.175 ± 0.011	VLT 8 m
Jul 13.151	20.183 ± 0.009	VLT 8 m
Jul 13.174	20.251 ± 0.085	ESO 1.5 m
Jul 13.328	20.470 ± 0.10	MJUO 61 cm
Jul 13.383	20.533 ± 0.016	VLT 8 m
Jul 13.395	20.460 ± 0.057	CASLEO 2.15 m
Jul 13.750	20.857 ± 0.088	SAAO 1 m
Jul 14.127	20.968 ± 0.025	VLT 8 m
Jul 14.287	20.991 ± 0.040	NTT 3.5 m
Jul 14.683	21.490 ± 0.27	MJUO 61 cm
Jul 14.764	21.201 ± 0.123	SAAO 1 m
Jul 16.403	21.420 ± 0.050	NTT 3.5 m
Jul 20.421	21.550 ± 0.050	NTT 3.5 m
Aug 02.533.....	21.584 ± 0.036	AAT 3.9 m
Aug 12.232.....	21.650 ± 0.030	VLT 8 m
Aug 16.320.....	21.750 ± 0.060	CTIO 0.9 m[a]
Aug 16.445.....	21.779 ± 0.041	AAT 3.9 m
V-Band Measurements		
Jul 13.156	20.523 ± 0.017	SAAO 1 m
Jul 13.158	20.516 ± 0.015	SAAO 1 m
Jul 13.405	20.852 ± 0.023	VLT 8 m
Jul 13.406	20.866 ± 0.028	VLT 8 m
Jul 14.157	21.290 ± 0.041	VLT 8 m
Jul 14.298	21.458 ± 0.053	VLT 8 m
Jul 14.787	21.795 ± 0.089	SAAO 1 m
Jul 20.433	22.065 ± 0.100	NTT 3.5 m
Aug 02.511.....	22.136 ± 0.042	AAT 3.9 m
Aug 16.471.....	22.305 ± 0.054	AAT 3.9 m
I-Band Measurements		
Jul 13.774	20.266 ± 0.082	SAAO 1 m
Jul 14.271	20.603 ± 0.078	NTT 3.5 m
Jul 14.810	20.933 ± 0.258	SAAO 1 m
Jul 20.439	20.950 ± 0.100	NTT 3.5 m
Aug 02.554.....	21.164 ± 0.165	AAT 3.9 m
Aug 16.414.....	21.420 ± 0.100	AAT 3.9 m

[a] Taken from Kemp & Halpern (1999).

ESO, and AAO. A log of all the observations used in this analysis along with the derived magnitudes of the OT are listed in Table 1. The measurements include the acquisition images taken for the spectroscopic observations with the ESO VLT shortly after the discovery of the OT (Vreeswijk et al. 2000).

2.1. *Astrometry and Photometry of the Optical Counterpart*

An astrometric solution of the field was carried out using 10 reference stars in the image (Fig. 1). Their coordinates, as taken from the USNO 2.0 catalog, which uses the *Hipparcos* frame of reference, are listed in Table 2. The pixel centroids of the reference stars were determined using two-dimensional Gaussian fits. These centroids were combined with the USNO coordinates to determine an astrometric solution of the field. The resulting position of the optical counterpart is R.A.(2000) = $22^h31^m53^s.061 \pm 0^s.011$, decl.(2000) = $-73°24'28''.58 \pm 0''.05$.

Since sky conditions deteriorated because of clouds just after the discovery observations of the OT, no standard star observations could be taken on that night. The images were calibrated through observations of the standard stars F203 and F209 (Menzies et al. 1989) taken on 1999 July 13 at SAAO. All the photometric measurements were carried out using the IRAF aperture photometry task PHOT. The photometry of a few secondary standards in the field (Fig. 1) was carried out using the standard star observations, and the photometry of all GRB observations was then performed via these secondary standards. Since only two standard stars were observed, the extinction correction due to differential air mass between the GRB and the standard star observations was not applied in the preliminary analysis (Bakos et al. 1999a, 1999b). Instead, the photometric measurements taken with the adjacent 50 cm telescope were used to get the extinction coefficients, which resulted in a correction of -0.075 mag in V, -0.06 mag in R, and -0.02 mag in I (this is consistent with the discrepancy pointed out by Kemp & Halpern 1999). Our final magnitudes of the secondary photometric standards are listed in Table 2, and Table 1 lists the derived magnitudes of the OT in different bands at different epochs, including one extra measurement reported by Kemp & Halpern (1999).

3. ANALYSIS

3.1. *The Light Curve in Different Wave Bands*

All the photometric measurements listed in Table 1 are also shown in Figures 2 and 3. The observed light curves in different bands clearly show a continuously changing slope, suggesting an additional component to the power-law decay of the OT, as first noted by Hjorth et al. (1999a). In an

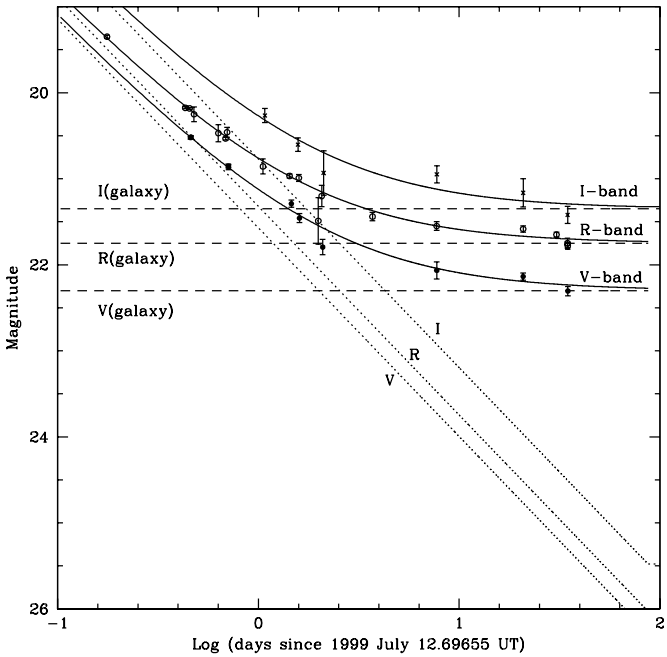

FIG. 2.—Observed light curves of GRB 990712 in different optical bands and the model fits assuming a power-law decay for the OT and the presence of an underlying galaxy. The *I*-band measurements are shown as asterisks, the *R*-band measurements are shown as open circles, and the *V*-band measurements are shown as filled circles. The magnitudes of the underlying galaxy in different bands are shown as horizontal dashed lines. The dotted lines show the decay characteristic of the OT, and the solid curves show the combined OT + galaxy. The derived slope of the power-law decay is $0.97 \pm {}^{0.05}_{0.02}$, and the magnitudes of the underlying galaxy are $V = 22.3 \pm 0.05$, $R = 21.75 \pm 0.05$, and $I = 21.35 \pm 0.05$.

TABLE 2

POSITIONS AND MAGNITUDES OF OT AND REFERENCE STARS AND MAGNITUDES OF SECONDARY STANDARDS

Number	R.A.(2000)	Decl.(2000)	X	Y	V	R	I
OT and Reference Stars 1–4							
OT.....	22 31 53.0614	−73 24 28.576	579.40	620.02	...	...	...
1	22 31 50.8933	−73 24 25.280	609.98	630.95	17.185	16.40	15.64
2	22 31 40.1507	−73 25 09.400	758.34	487.54	16.975	16.65	16.29
3	22 31 49.7413	−73 26 09.250	624.22	294.44	16.455	15.97	15.50
4	22 32 18.6200	−73 24 09.920	224.05	680.45	15.905	15.27	14.65
Additional Reference Stars Used for Astrometry							
5	22 31 49.3380	−73 24 53.130	631.68	537.68	...	...	...
6	22 32 02.5307	−73 25 27.980	446.48	427.78	...	...	...
7	22 32 00.6387	−73 23 20.810	474.52	839.78	...	...	...
8	22 31 37.5760	−73 23 34.160	794.42	796.29	...	...	...
9	22 32 21.9453	−73 24 27.680	179.47	623.97	...	...	...
10	22 32 16.1573	−73 24 55.230	259.72	535.90	...	...	...

NOTE.—Units of right ascension are hours, minutes, and seconds, and units of declination are degrees, arcminutes, and arcseconds. The magnitudes have typical uncertainties of 0.01 mag.

approach similar to the one followed by Hjorth et al. (1999b), we have fitted this additional component in two ways: with (1) an underlying galaxy of constant brightness and (2) an underlying galaxy plus a supernova similar to GRB 980425, appropriately scaled to the redshift of GRB 990712.

First, a power-law decline of the form $f(t) \propto t^{-\alpha}$ for the OT and a constant contribution from the background galaxy were used to fit the observed light curves simultaneously in different bands, with the same slope for all the bands. The resultant slope is 0.97, and the total χ^2 is 47 for 39 degrees of freedom (dof) (relaxing the condition of the same slope in different bands does not alter the fit parameters significantly). The total χ^2 is, however, fairly flat (between 44 and 52) for any value of α between 0.95 and 1.02, beyond which the total χ^2 increases rapidly. Figure 2 shows the best fit to the light curves. The derived magnitudes of the underlying galaxy are not very sensitive to the exact value of α and are found to be $V = 22.3 \pm 0.05$, $R = 21.75 \pm 0.05$, and $I = 21.35 \pm 0.05$, where the uncertainties represent the variation of the derived magnitudes as a result of changing α between 0.95 and 1.02.

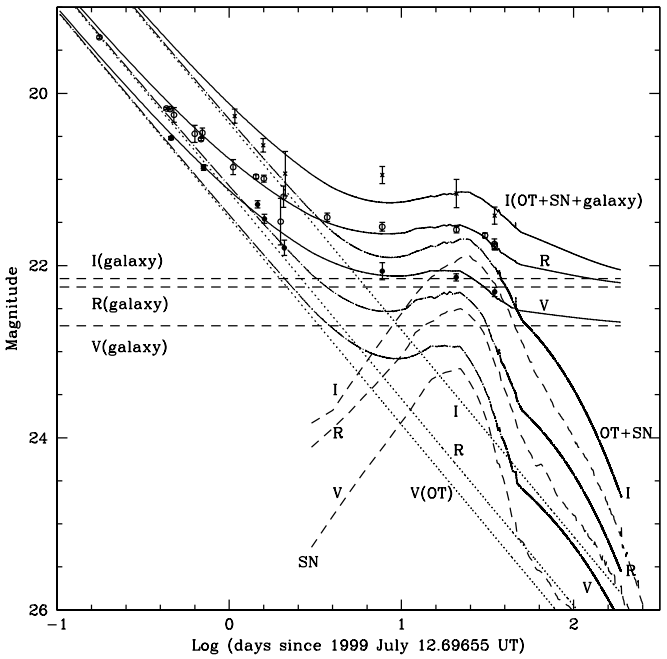

FIG. 3.—Observed light curves of GRB 990712 in different optical bands and the fits to the light curves assuming a power-law decay for the OT, an underlying galaxy, and an underlying supernova whose brightness is assumed to be identical to that of GRB 980425 scaled appropriately to the redshift of GRB 990712. The symbols used are the same as in Fig. 2. In addition, the light curves of the supernova (scaled as explained before) in different bands are shown as dashed lines, the light curves of the SN+OT are shown as dot-dashed curves, and the light curves of the OT+SN+galaxy are shown as solid curves. The derived slope of the power-law decay is $0.96 \pm {}^{0.05}_{0.02}$, and the magnitudes of the underlying galaxy are $V = 22.7 \pm 0.05$, $R = 22.25 \pm 0.05$, and $I = 22.15 \pm 0.05$.

One possible consequence of the massive star model for the GRB is that one should observe an underlying supernova in the light curve of an OT. The hypothesis of a physical connection of a GRB with a supernova (SN), first suggested by the discovery of a peculiar Type Ic SN in the error box of GRB 980425 (Galama et al. 1998; Iwamoto et al. 1998), has been strengthened further by recent observations of other GRBs. Castro-Tirado & Gorosabel (1999) suggested that the light curve of GRB 980326 resembled that of a SN, and indeed Bloom et al. (1999) showed that the late-time light curve of GRB 980326 can be explained by an underlying 1998bw-type SN at a redshift of around unity. For the afterglow of GRB 970228, Reichart (1999) and Galama et al. (2000) find that a power-law decay plus SN 1998bw light curve redshifted to the distance of the burst, $z = 0.695$ (Djorgovski et al. 1999), fits the observed light curve very well. In light of these new findings, we have also fitted the observed light curve of GRB 990712 assuming the presence of an underlying supernova.

In order to determine the contribution of the underlying supernova, we first calculate the expected V, R, and I magnitudes of SN 1998bw, placing it at the redshift of GRB 990712, $z = 0.434$. This includes wavelength shifting and time profile stretching (both by a factor of $1 + z$) and rescaling the magnitudes for a distance corresponding to $z = 0.434$, assuming $\Omega_0 = 0.2$. To account for the wavelength shift correctly, we interpolate the redshifted $UBVRI$ broadband flux spectrum of the SN for each bin in time

with a spline fit, obtain the V, R, and I fluxes at their effective wavelengths, and convert these back to obtain magnitudes in the observer's frame (Fukugita et al. 1995). The resultant SN light curves in different bands are shown at the bottom of Figure 3. In order to fit the GRB light curve, the SN flux is subtracted from the observed GRB flux, and the residual fluxes are assumed to be due to the OT and the underlying galaxy. The procedure outlined earlier is then used to fit the light curves. The χ^2 in this case is 52 for 42 dof, which is clearly higher than the model without the supernova. The resulting slope of the decay is 0.96, which is quite similar, but the magnitudes of the underlying galaxy are fainter: $V = 22.7 \pm 0.05$, $R = 22.25 \pm 0.05$, and $I = 22.15 \pm 0.05$. The brightness of the OT of the GRB at a given time is also slightly lower, but the combined brightness of the OT and the underlying supernova (which is the quantity that can be measured if the OT can be resolved from the galaxy) is higher than the brightness of the OT in the absence of an underlying supernova.

It is important to note, however, that there is no evidence that the SNe possibly underlying the GRB afterglows have the same brightness or the same decay behavior. Our assumption that the underlying supernova is identical to SN 1998bw is dictated by two reasons. First, this is the only SN associated with a GRB whose light curve has been monitored extensively. Second, the number of data points in our light curves does not allow us to vary the characteristics of the underlying SN light curve. So the fact that the χ^2 is higher in this case can be misleading since the true underlying supernova may be different from that of SN 1998bw, making the resultant χ^2 higher for our simplified model. This χ^2 analysis indicates that either GRB 990712 is not associated with an underlying supernova or the underlying supernova is much fainter than the supernova associated with GRB 980425. However, the qualitative conclusion that the galaxy is expected to be fainter and the OT plus the SN is expected to be brighter in the presence of an underlying supernova is unlikely to change. Hence, late-time *HST* observations, in which the OT is well resolved so that the brightness of the OT and the galaxy can be estimated separately, or late-time ground-based observations, when the brightness of the OT is negligible, would greatly help in determining the presence of an underlying supernova.

In both of the above scenarios (i.e., with and without an underlying supernova), the power-law index of the decay α is about 1, making it one of the slowest decline rates of all the OTs observed so far. Since $\alpha \leq 1$ would lead to a divergence of the total energy integrated over time, the slope must steepen at later times. This has been observed for GRB 990510, which declined with $\alpha = 0.82$ at early times, later steepening with time (Harrison et al. 1999). Power-law decays are thought to arise from electrons shocked by the relativistic expansion of the debris into the ambient medium. In such a case, the information on the change of slope can be used to derive information on the cooling rate of the electrons in the postshock region (see, e.g., Wijers et al. 1997; Sari, Piran, & Narayan 1998; Livio & Waxman 1999).

3.2. *Spectral Energy Distribution of the OT*

If the OT emission is due to the synchrotron radiation from the swept-up electrons in the postshock region, then its energy distribution is expected to be of the general form $f_\nu \propto t^{-\alpha}\nu^{\beta}$. In such a case, one expects a relationship between the power-law index of the energy distribution of the electrons p, the spectral slope β, and the decay constant α (Sari et al. 1998). One must distinguish two cases: (1) both the peak frequency ν_m and the cooling frequency ν_c are below the optical/IR wave band, in which case $p = (4\alpha + 2)/3 = 1.97 \pm 0.04$ and $\beta = -p/2 = -0.99 \pm 0.02$, and (2) ν_m has passed the optical/IR wave band, but ν_c has not yet done so, in which case $p = (4\alpha + 3)/3 = 2.31 \pm 0.04$ and $\beta = -(p - 1)/2 = -0.66 \pm 0.02$.

We can now compare the theoretically expected spectral slope (β) with the observed one. Although perhaps best determined by the spectroscopic measurements, our light-curve analysis provides magnitudes of the OT in different bands, which can be used directly to derive β. We should note here that the brightness of the underlying galaxy and the possible contamination by an underlying supernova make the determination of the magnitudes of the OT less reliable at later times, and our value of α is most likely dominated by the early part of the light curve, when the OT was bright. Furthermore, α was kept fixed in *all* the bands for the entire period of our observations, which implies that we cannot detect any spectral *evolution* of the OT. The SYNPHOT/CALCPHOT task in IRAF was used to determine the V–R and R–I values for a range of β values, which were then compared with the colors derived from the light-curve analysis to determine the spectral slopes. The V–R color implies a spectral slope of -1.8 ± 0.5, and the R–I color implies a spectral slope of -0.7 ± 0.1. Thus, the slope derived from the V and R bands is closer to the former case mentioned above, and the slope derived from the R and I bands is closer to the latter case. This is roughly consistent with the theoretical expectations and implies that, in the early part of the light curve, ν_m has passed the V, R, and I bands but ν_c has not passed the I band.

3.3. *The Background Galaxy*

The inferred magnitudes for an underlying galaxy suggest that the galaxy is relatively bright compared to the OT, and it may be possible to see the host galaxy directly in the images. The New Technology Telescope (NTT) images taken about 8 days after the burst had the best seeing ($\sim 1''$), and the R images indeed show some hint of a slight extension. To investigate this further, all the images taken in B, V, R, and I bands were co-added, giving rise to a single deep image of a total integration time of 40 minutes. From this combined image, we constructed a model point-spread function (PSF) from a few isolated bright stars in the field using IRAF/DAOPHOT. This model PSF was used to subtract the point-source contribution from the OT. The PSF-subtracted image shows some residual distribution elongated in the eastward direction of the OT over a total of about $2''$, which is probably the contribution of the underlying galaxy. Thus, *HST* observations would show the detailed structure of the galaxy (Fruchter et al. 2000).

The derived magnitudes of the underlying galaxy were used to calculate its luminosity. The GRB is at a Galactic latitude and longitude of $-40°$ and $315°$, respectively. The extinction models of Burstein & Heiles (1982) and Schlegel, Finkbeiner, & Davis (1998) yield $E(B-V)$ of 0.015 and 0.033, respectively, for the position of the GRB. This extinction is small and similar to SN 1998bw, which is neglected in our analysis. To derive the luminosity of the host galaxy, we use a redshift of $z = 0.434$, which, for $H_0 = 70$ km s^{-1} and $\Omega = 0.2$, corresponds to a luminosity distance of 2160

Mpc and a distance modulus of 41.67 mag. Applying the K-correction for $z = 0.434$, the inferred luminosity of the galaxy is of the order of L_* (depending on the presence of an underlying supernova), where L_* corresponds to the luminosity of a typical galaxy at the "knee" of the observed galaxy luminosity function (see, e.g., Lilly et al. 1999).

If we exclude SN 1998bw (which is not only "nearby" [$z = 0.008$] but for which the energy released in gamma rays is much smaller than for any other GRB), then GRB 990712 is the closest "cosmological" GRB, and the apparent magnitude of its host galaxy is the brightest among all the GRB host galaxies observed so far. Compared to the host galaxy of GRB 990713, which is the next brightest, the host galaxy of GRB 990712 is about 0.25 mag brighter in R if there is an underlying supernova, and more than a magnitude brighter if there is no underlying supernova.

We dedicate this paper to the memory of our colleague and friend Jan van Paradijs, who passed away as a result of an illness on 1999 November 2 during the final stages of the preparation of this manuscript. Jan received several awards for his fundamental contributions in this field, including the 1998 Rossi prize of the American Astronomical Society. We will sorely miss his contagious enthusiasm, his brilliant insights, and his benevolent personality.

This project is partly supported by the Chilean Fondecyt Project 3990024 and the Danish Natural Science Research Council (SNF). M. Dominik is supported by a Marie Curie Fellowship (ERBFMBICT972457).

REFERENCES

Albrow, M. D., et al. 1998, ApJ, 509, 687
Bakos, G., et al. 1999a, GCN Circ. 387 (http://gcn.gsfc.nasa.gov/gcn/gcn3/387.gcn3)
———. 1999b, IAU Circ. 7255
Bloom, J. S., et al. 1999, Nature, 401, 453
Bloom, J. S., Sigurdsson, S., & Pols, O. R. 1999, MNRAS, 305, 763
Burstein, D., & Heiles, C. 1982, AJ, 87, 1165
Castro-Tirado, A. J., & Gorosabel, J. 1999, A&AS, 138, 449
Costa, E., et al. 1997, Nature, 387, 783
Djorgovski, S. G., et al. 1999 GCN Circ. 289 (http://gcn.gsfc.nasa.gov/gcn/gcn3/289.gcn3)
Eichler, D., Livio, M., Piran, T., & Schramm, D. N. 1989, Nature, 340, 126
Fishman, G. J. 1999, in Proc. STScI Symp., Supernovae and Gamma-Ray Bursts, ed. M. Livio, K. C. Sahu, & N. Panagia (Baltimore: STScI), in press
Fruchter, A., et al. 1999, ApJ, 519, L13
———. 2000, in preparation
Fukugita, M., Shimasaku, K., & Ichikawa, R. 1995, PASP, 107, 945
Galama, T. J. 1998, Nature, 395, 670
———. 1999, GCN Circ. 388 (http://gcn.gsfc.nasa.gov/gcn/gcn3/388.gcn3)
———. 2000, ApJ, 536, 185
Harrison, F. A., et al. 1999, ApJ, 523, 121
Heisse, J., et al. 1999, IAU Circ. 7221
Hjorth, J., et al. 1999a, GCN Circ. 389 (http://gcn.gsfc.nasa.gov/gcn/gcn3/389.gcn3)
———. 1999b, GCN Circ. 403 (http://gcn.gsfc.nasa.gov/gcn/gcn3/403.gcn3)
———. 2000, ApJ, submitted (astro-ph/0003383)
Iwamoto, K., et al. 1998, Nature, 395, 672
Kemp, J., & Halpern, J. 1999, GCN Circ. 402 (http://gcn.gsfc.nasa.gov/gcn/gcn3/402.gcn3)
Kouveliotou, C., et al. 1995, in AIP Conf. Proc. 384, 3d Huntsville Symp. on Gamma Ray Bursts, ed. C. Kouveliotou, M. F. Briggs, & G. J. Fishman (New York: AIP), 42
Kulkarni, S. R., et al. 1998, Nature, 393, 35
Lilly, S. J., et al. 1999, ApJ, 518, 641
Livio, M., & Waxman, E. 1999, ApJ, submitted (astro-ph/9911160)
Menzies, J. W., Cousins, A. W. J., Banfield, R. M., & Laing, J. D. 1989, SAAO Circ. 13, 1
Mészáros, P., & Rees, M. J. 1997, ApJ, 476, 232
Metzger, M. R., et al. 1997, Nature, 387, 879
Narayan, R., Paczyński, B., & Piran, T. 1992, ApJ, 395, L83
Paczyński, B. 1998, ApJ, 494, L45
Paczyński, B., & Rhoads, J. E. 1993, ApJ, 418, L5
Reichart, D. E. 1999, ApJ, 521, L111
Sahu, K. C., et al. 1997a, Nature, 387, 476
———. 1997b, ApJ, 489, L127
Sari, R., Piran, T., & Narayan, R. 1998, ApJ, 497, L17
Schlegel, D., Finkbeiner, D., & Davis, M. 1998, ApJ, 500, 525
van Paradijs, J., et al. 1997, Nature, 386, 686
Vreeswijk, P. M., et al. 2000, in preparation
Wijers, R. A. M. J., Rees, M. J., & Mészáros, P. 1997, MNRAS, 288, L51
Woosley, S. E. 1996, in AIP Conf. Proc. 384, Gamma-Ray Bursts: 3d Huntsville Symp., ed. C. Kouveliotou, M. Briggs, & G. Fishman (New York: AIP), 709